# Controlling spatiotemporal chemical chaos using delayed feedback

P. Parmananda
*Facultad de Ciencias, Universidad Autonoma del Estado de Morelos, Avenida Universidad 1001, Col. Chamilpa, Cuernavaca, Morelos, Mexico*

J. L. Hudson
*Department of Chemical Engineering, Thornton Hall, University of Virginia, Charlottesville, Virginia 22903-2442*
(Received 18 January 2001; published 7 August 2001)

Control of chemical chaos in a spatially extended system mimicking CO oxidation on a Pt(110) single-crystal surface is achieved using delayed feedback techniques. For appropriate parameter values the uncontrolled model system exhibits both amplitude and phase turbulence. Superimposing a delayed feedback on the natural dynamics, suppression of spatiotemporal complexity is attained via stabilization of ordered states consisting of stable patterns.

DOI: 10.1103/PhysRevE.64.037201 PACS number(s): 05.45.Gg, 05.45.Jn

## I. INTRODUCTION

The suppression of turbulent behavior observed in spatially extended nonlinear systems is of much practical interest. The growing interest in this field stems from the pioneering work done by Ott *et al.* [1] in controlling chaos. Since then temporal chaos has been controlled in various experimental systems [2–5]. These efforts have been naturally extended to tame complex behavior observed in distributed dynamical systems [6–10]. This control of spatiotemporal chaos is an extremely complicated problem due to the existence of numerous unstable spatial modes. However, it deserves to be addressed because of its numerous applications in plasma, laser devices, and various chemical and biological systems where both spatial and temporal dependencies need to be considered.

In this report we propose using delayed feedback techniques [11] to control high-dimensional chaotic behavior. In Sec. II, we describe the model system chosen for implementation of the delayed feedback control method. Numerical results indicating successful suppression of complexity in the model system are presented in Sec. III along with an evaluation of the control techniques.

## II. NUMERICAL MODEL FOR CO-OXIDATION

We choose the following model with one spatial dimension used for the description of CO oxidation on a Pt(110) single-crystal surface under ultrahigh vacuum conditions [12,13]. The CO oxidation on Pt (110) proceeds via the Langmuir-Hinshelwood mechanism and associated surface structural changes. The underlying dynamics are determined by the surface coverages of CO and O and their interactions with the surface structure $v$. Spatial coupling of adjacent regions on the catalyst is provided by the surface diffusion of CO [12]. Since the CO and O coverages are always strictly anticorrelated for realistic parameters, they can be combined to a single coverage variable $u$ that exhibits an *S*-shaped nullcline. For efficient numerical integration this nullcline can be simplified to a *Z*-shaped nullcline resulting in the following system of equations after rescaling of space and time:

$$\partial_t u = -\frac{u(u-1)}{\epsilon}\left(u - \frac{v+b}{a}\right) + D\nabla^2 u, \tag{1}$$

$$\partial_t v = f(u) - v, \tag{2}$$

where $u$ and $v$ are activator and inhibitor variables, respectively. The continuous and differentiable function $f(u)$ exhibits the following threshold values (''delayed inhibitor production''):

$$u < 1/3 \rightarrow f(u) = 0;$$

$$1/3 \leqslant u \leqslant 1 \rightarrow f(u) = 1 - 6.75u(u-1)^2;$$

$$u > 1 \rightarrow f(u) = 1.$$

The function $f(u)$ was fitted to experimental low-energy electron diffraction and scanning tunneling microscopy data such that the simulations are consistent with experimental observations [14].

Under appropriate parameter values in one spatial dimension, the model system exhibits transition to spatiotemporal chaos via backfiring of pulses. A bifurcation analysis reveals that the model system may exhibit traveling pulse behavior, amplitude turbulence, and phase turbulence [12,13]. To integrate associated PDE's [Eqs. (1) and (2)] the system size was chosen to be 100 dimensionless units and then divided into 200 grid elements for simulation using explicit integration algorithm with constant time and space (100/200) steps subjected to periodic boundary conditions.

## III. NUMERICAL RESULTS

The spatially extended system exhibits amplitude turbulence dynamics for the following set of parameter values: $a = 0.84$, $\epsilon = 0.12$, $b = -0.045$, and $D = 1/5.2$. Results from three distinct control strategies are presented in different sections.

### A. Local feedback superimposed on one site

In this case, one of the sites of the spatially extended system is perturbed. The feedback involves sampling the

 

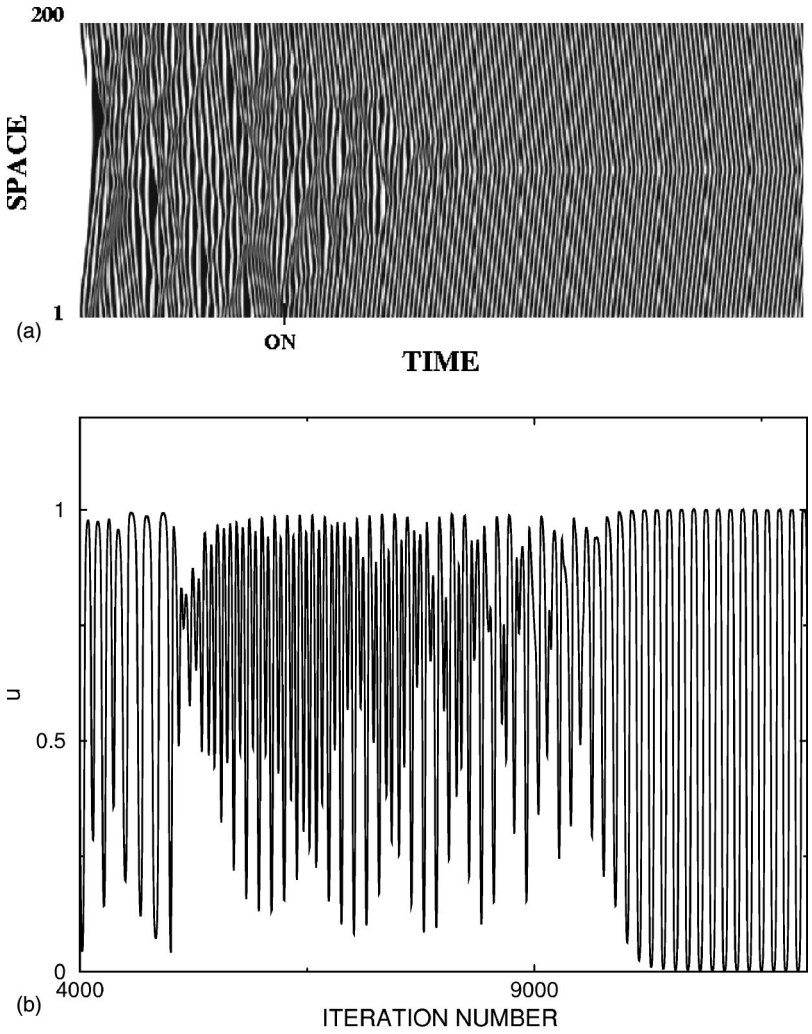


FIG. 1. Control of chemical complexity via stabilization of traveling pulse train solutions for the spatially extended system using the control as discussed in Sec. III A. The system parameters are $a=0.84$, $\epsilon=0.12$, $b=-0.045$, and $D=1/5.2$ and the control parameters are $\gamma=-0.8$ and $\tau=125$ (No. of integration steps). (a) Space-time portrait prior and subsequent to (indicated by ''ON'') implementation of the control signal. Every 20th step is plotted along the time axis. It illustrates induction and subsequent propagation of global order by virtue of a local perturbation. (b) The local time series of the 100th cell prior and subsequent to the implementation of the control. The controlled time series is a period-one oscillation indicating inception of order.

time series for one of the 200 coupled oscillators at two different times $(t-\tau,\tau)$ and superimposing the difference onto the evolution equation of the same oscillator

$$\partial_t u = -\frac{-1u(u-1)}{\epsilon}\left(u-\frac{v+b}{a}\right)+D\nabla^2 u + \gamma[u(t)-u(t-\tau)]\delta_{i1}, \tag{3}$$

$$\partial_t v = f(u)-v. \tag{4}$$

The appropriate $\tau$ is chosen by observing the uncontrolled time series of the global average $[(1/N)\Sigma_{i=1}^{N}u_i(t)]$. By constructing a temporal return map ($T_n$ vs $T_{n-1}$) and monitoring the time elapsed ($T$) between successive extrema in the vicinity of the line of identity and doing a linear least-squares fit, one can approximate the appropriate $\tau=T$ [11]. The $\tau$ calculated using this temporal return map merely provides a first-order estimate for the appropriate delay ($\tau$) and perhaps could be obtained using trial and error. The $\delta_{i1}$ part of the feedback ensures that only the first site (site No. 1) is being perturbed. Figure 1(a) shows the space-time plot for the ex-

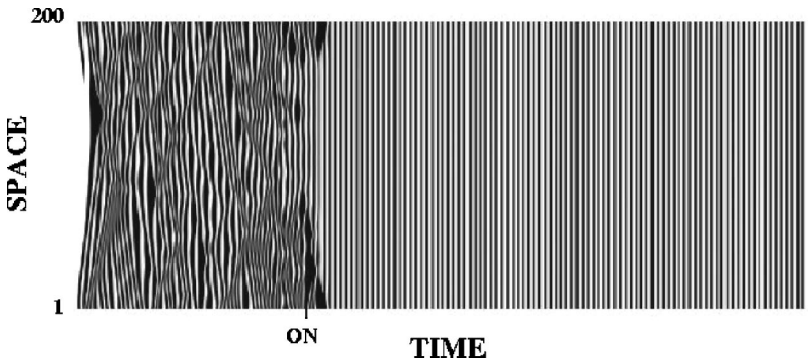


FIG. 2. Space-time portrait prior and subsequent to (indicated by ON) implementation of the local feedback indicating suppression of spatiotemporal chemical chaos via stabilization of a spatially homogeneous and temporally periodic state for the spatially extended system. The system parameters are same as Fig. 1 and the control parameters are $\gamma=-0.2$ and $\tau=125$. Every 20th step is plotted along the time axis.

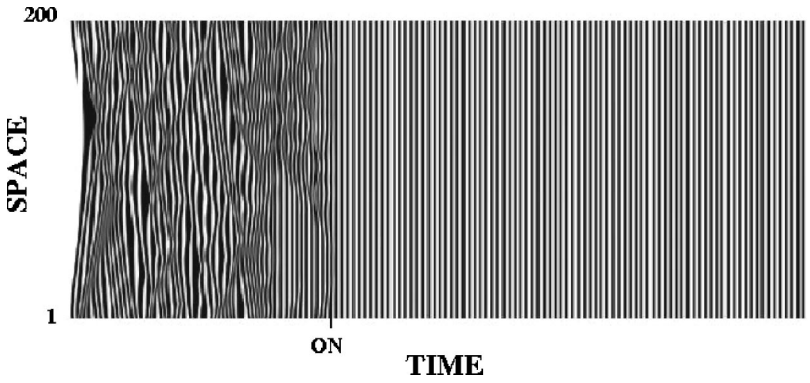


FIG. 3. Space-time portrait prior and subsequent to (indicated by ON) implementation of the global feedback indicating control of chemical chaos via stabilization of a spatially homogeneous and temporally periodic state. The system parameters are same as Fig. 1 and the control parameters are $\gamma=-0.11$ and $\tau=125$. Every 20th step is plotted along the time axis.

tended system under the effect of this local feedback. The model dynamics exhibit an inception of order at the point of stimulation and its subsequent propagation, up until complete suppression of spatiotemporal complexity, is achieved. The stabilized state consists of pulse trains traversing the excitable media [15]. Figure 1(b) shows the local time series for the site No. 100 furthest (since we have periodic boundary conditions) from the point of stimulation. It indicates control of chaos locally via conversion to a period-one oscillatory state. The control feedback to the perturbed site although, small, remains nonzero. The smallest value of $\gamma$ for which global suppression of complexity could be achieved was $\gamma=0.8$. It is a powerful technique since for the appropriate choice of $\tau$ and $\gamma$, one can achieve global order via nonzero local perturbations.

### B. Local feedback superimposed on all sites

Feedback of this type involves taking the difference between the instantaneous local value $[u_i(t)]$ and the past value of one of the predesignated sites [site No. 1; $u_1(t-\tau)$] and superimposing it on all sites. Under the influence of this feedback, the controlled dynamics are represented by

$$\partial_t u = -\frac{-1u(u-1)}{\epsilon}\left(u-\frac{v+b}{a}\right)+D\nabla^2 u + \gamma[u_i(t)-u_1(t-\tau)], \tag{5}$$

$$\partial_t v = f(u)-v. \tag{6}$$

For the control of the type in Eqs. (5) and (6), $\tau$ is chosen as described in the previous section. Figure 2 shows the gray-coded space-time evolution of the model system. Under the influence of an oscillating feedback, the turbulent dynamics are converted to spatially homogeneous yet temporally periodic solutions. This is different from the traveling pulse train solutions stabilized in the previous section. Using different values of $\gamma$ and $\tau$ a whole spectrum of periodic dynamics can be targeted and subsequently stabilized.

### C. Global feedback superimposed on all sites

This involves continuous computation of the global average $[(1/N)\Sigma_{i=1}^{N}u_i(t)]$ of an observable at two discreet times $(t-\tau,t)$ and subsequently superimposing it on to the dynamical evolution of each site in the model system:

$$\partial_t u = -\frac{-1u(u-1)}{\epsilon}\left(u-\frac{v+b}{a}\right)+D\nabla^2 u + \gamma\left[\frac{1}{N}\sum_{i=1}^{N}u_i(t)-\frac{1}{N}\sum_{i=1}^{N}u_i(t-\tau)\right], \tag{7}$$

$$\partial_t v = f(u)-v. \tag{8}$$

For the control of the type in Eqs. (7) and (8), $\tau$ is chosen as described in the Sec. III A. Figure 3 shows the space-time plot for the extended system indicating the control of turbulent dynamics. This technique could be implemented in experiments as the global observables required to compute the controlling feedback are easily accessible.

Numerical results involving different methods of implementations of delayed feedbacks indicate successful stabilization of naturally unstable periodic dynamics. Upon suppression of complexity, the control signal, although small (less than 10% remains nonvanishing. The strategy of Sec. III A involves the induction of global order via local perturbations. This is applicable to experimental situations and moreover is of interest in an information theoretic context in biology. Local temporal information of biological relevance could be encoded in a meaningful [15] ordered spatial pattern that creates corresponding temporal signals at distinct sites. Furthermore, pattern formation inside a cell could act as a biologically relevant encoding mechanism to transfer extracellular signals to targeted sites of biochemical action. For the control strategy of Sec. III B the correctional feedback superimposed on a site is related to the local dynamics at that site. It is possible to envisage a setup (for example, using optical illumination as the control parameter) where the effect of control on different sites of an extended system is a function of the local state of individual sites making it relevant to experimental situations. The strategy of Sec. III C involves using experimentally accessible global observables and hence makes it a suitable candidate in efforts to tame spatiotemporal chaos in real systems.

## ACKNOWLEDGMENTS

This work has been supported by NSF and CONACyT (Mexico).

[1] E. Ott, C. Grebogi, and J.A. Yorke, Phys. Rev. Lett. **64**, 1196 (1990).
[2] W.L. Ditto, S.N. Rauseo, and M.L. Spano, Phys. Rev. Lett. **65**, 3211 (1990).
[3] E.R. Hunt, Phys. Rev. Lett. **67**, 1953 (1991).
[4] R. Roy, T.W. Murphy, Jr., T.D. Maier, Z. Gills, and E.R. Hunt, Phys. Rev. Lett. **68**, 1259 (1992).
[5] V. Petrov, V. Gáspár, J. Masere, and K. Showalter, Nature (London) **361**, 240 (1993).
[6] Hu Gang and Qu Zhilin, Phys. Rev. Lett. **72**, 68 (1994).
[7] Ditza Auerbach, Phys. Rev. Lett. **72**, 1184 (1994).
[8] I. Aranson, H. Levine, and L. Tsimring, Phys. Rev. Lett. **72**, 2561 (1994).
[9] D. Battogtokh and A. Mikhailov, Physica D **90**, 84 (1996).
[10] P. Parmananda, M. Hildebrand, and M. Eiswirth, Phys. Rev. E **56**, 239 (1997).
[11] K. Pyragas, Phys. Lett. A **170**, 421 (1992).
[12] M. Bär, C. Zülicke, M. Eiswirth, and G. Ertl, J. Chem. Phys. **100**, 1202 (1994).
[13] M. Bär and M. Eiswirth, Phys. Rev. E **48**, R1635 (1993).
[14] G. Ertl, Science **254**, 1750, (1991).
[15] G. Baier, S. Sahle, J.-P. Chen, and A.A. Hoff, J. Chem. Phys. **110**, 3251 (1999).